struktur einiger Übergänge ($M = -1/2 \rightarrow +1/2$ und $-3/2 \rightarrow -1/2$) bei 9 GHz, 77 K berichtet, während andere Übergänge (fast) keine Struktur zeigen. Die Beobachtung der shfs im EPR-Spektrum $B \parallel [001]$ in Abhängigkeit vom Mikrowellen-Magnetfeld B_1 (Sättigungsverhalten), vom äußeren Magnetfeld B (bei 9 GHz und 35 GHz) und vom Elektronenspin M (innerhalb der Hauptspektren $\Delta M = 1$, $\Delta m = 0$) läßt sich mit theoretischen Vorstellungen nach[12] und den Konstanten in Gl. (6a), (6b) befriedigend erklären. Die Wechselwirkung des Elektronenspins von Eu^{2+} mit den Kernspins der nächsten Nachbarn (F^-) führt zu einer Aufspaltung der Energieniveaus der Elektronen. Diese Energieaufspaltung ist abhängig vom Elektronenspin M und vom äußeren Magnetfeld B [s. Gl. (9)]. Sie bewirkt eine Verbreiterung oder Strukturierung der Hyperfeinlinien im EPR-Spektrum. Bei 9 GHz sind nur wenige Linien strukturiert[1], bei 35 GHz dagegen fast alle [s. Abb. (11b)].

Eine Strukturierung tritt dann auf, wenn die Aufspaltungsenergie der beteiligten Niveaus nicht zu sehr von der Zeeman-Aufspaltung abweicht [Gl. (16)] und die Temperatur nicht zu hoch ist. Dieses Ergebnis, die geringe Auflösung an den Linien I, II bei 35 GHz (Abschnitt Va) und die Betrachtung der Linienbreiten (Abschnitt Vd) legen die Vermutung nahe, daß bei Berechnung der Aufspaltung δ nach Gl. (9) nicht berücksichtigte (thermisch bedingte) statistische Schwankungen der Wechselwirkungsparameter T eine Rolle spielen.

Die einzelnen Komponenten der shfs zeigen unterschiedliches Sättigungsverhalten (die Zentrallinie sättigt am stärksten). Nur deshalb sind im gesättigten Spektrum bei 9 GHz, 77 K mehr als 1 Nebenlinienpaar [1] und im Spektrum bei 35 GHz, 140 K [Abb. (11b)] überhaupt Nebenlinien zu sehen.

Unser Dank gilt dem Landesamt für Forschung des Landes Nordrhein-Westfalen und der Deutschen Forschungsgemeinschaft für die zur Verfügung gestellten Meßeinrichtungen und Herrn Dipl.-Phys. H. Vollmer für viele nützliche Diskussionen. Herrn Professor Dr. J. Jaumann, Universität zu Köln, danken wir für die im ersten Stadium der Messungen gewährte Unterstützung.

Rotational and Vibrational Excitation of H_2 by Slow Electron Impact

F. Linder and H. Schmidt

Fachbereich Physik der Universität Trier-Kaiserslautern

(Z. Naturforsch. **26 a**, 1603—1617 [1971]; received 1 July 1971)

In a beam experiment the processes of elastic scattering, pure rotational excitation and deexcitation, pure vibrational excitation, and simultaneous rotational-vibrational excitation have been investigated for e-H_2 scattering in the energy range from 0.3 eV to about 15 eV. Differential and integral cross sections have been determined in arbitrary units and calibrated on an absolute scale by normalization to absolute total cross sections. The results are discussed in terms of superposition of direct scattering, shape resonance and Feshbach resonance scattering and are compared with recent theoretical investigations. The cross sections for rotational and vibrational excitation, which are generally small for direct scattering, are greatly enhanced by a broad shape resonance near 3 eV and by Feshbach resonances around 12 eV. Characteristic differences in the excitation mechanisms are discussed.

Introduction

The $e - H_2$ system is one of the most interesting systems in atomic collision physics, both from theoretical and from experimental point of view. It is simple enough to allow ab-initio calculations for $e - H_2$ collision processes. Experimentally, the H_2 molecule is the most favourable example to carry out a detailed and quantitative investigation of electron molecule collision processes. In this work, emphasis is laid on the study of excitation mechanisms for rotational and vibrational excitation processes of H_2 by slow electron impact. Some general results should be representative for other diatomic molecules.

The importance of resonances for vibrational excitaton of H_2 has been shown in earlier measure-

Reprints request to Dr. F. Linder, NOAA Environmental Research Laboratories, *Boulder, Colorado 80302*, USA.

ments [1–5]. In these experiments most effort has been directed to the study of properties of resonances like energy position, half width, configuration, and branching ratios. Other experiments have yielded cross sections for vibrational excitation of H_2 outside the resonance region [6, 7]. All these measurements do not separate rotational excitation processes from pure vibrational excitation processes. The first beam experiment [8], in which rotational transitions of H_2 by slow electron impact were observed separately, removed large discrepancies in the understanding of the pure rotational excitation process, which had existed in theory and experiment at that time. The measurements have been extended to pure vibrational and simultaneous rotational and vibrational excitation [9]. By using a simple theoretical model, ABRAM and HERZENBERG [10] were able to show that at energies around 3 eV all these processes are strongly dominated by a broad shape resonance of $^2\Sigma_u^+$-configuration.

Further experimental information on rotational and vibrational excitation of H_2 is provided by electron swarm experiments [11]. While beam experiments mainly cover the energy range from about 1 eV to higher energies and are more valid to find out details of the scattering process, swarm experiments give very useful informations at very low energies. In recent experiments performed by CROMPTON et al. [12, 13] careful measurements on rotational and vibrational excitation of H_2 have been carried out for energies below 1 eV. In the present work, the beam measurements for rotational excitation have been extended down to a collision energy of 0.3 eV in order to get a range of overlap for both complementary methods.

The theory of $e - H_2$ scattering at low energies has been further worked out during the last years by several groups [14–19]. Extensive ab-initio calculations including polarization and exchange effects have been carried out for elastic scattering and rotational excitation. Recently the calculations have been extended to vibrational excitation [18].

In view of the progress in theory it is the purpose of the present paper to provide more accurate and more complete experimental data, especially with respect to angular distribution measurements and to the determination of absolute cross sections. The new experimental data are compared with recent theoretical results. Secondly, the measurements of rotational and vibrational excitation have been extended to energies above 10 eV where Feshbach resonances become important for the excitation processes. In the energy range measured three excitation mechanisms can be distinguished: excitation by a shape resonance, by a Feshbach resonance, and by normal direct scattering. Characteristic differences are found which are discussed in detail.

Experimental Procedures

The crossed beam apparatus and the electron spectrometer have been described in detail in earlier papers [3, 20]. An electron gun with a 127° electrostatic energy selector produces a beam of monochromatic electrons which is crossed at right angles with a molecular beam. The electrons which are scattered from the scattering centre into a certain solid angle are collected by an acceptor system and energy selected by a second 127° electrostatic energy analyzer. The collector system can be rotated from 0° to 120°. The scattered electrons are detected with a multiplier and conventional pulse counting electronics. The pulses are stored in

[1] G. J. SCHULZ, Phys. Rev. **135**, A 988 [1964].
[2] M. G. MENENDEZ and HELEN K. HOLT, J. Chem. Phys. **45**, 2743 [1966].
[3] H. EHRHARDT, L. LANGHANS, F. LINDER, and H. S. TAYLOR, Phys. Rev. **173**, 222 [1968].
[4] J. COMER and F. H. READ, J. Phys. B **4**, 368 [1971].
[5] A. WEINGARTSHOFER, H. EHRHARDT, V. HERMANN, and F. LINDER, Phys. Rev. **A 2**, 294 [1970].
[6] S. TRAJMAR, D. G. TRUHLAR, and J. K. RICE, J. Chem. Phys. **52**, 4502 [1970]. — S. TRAJMAR, D. G. TRUHLAR, J. K. RICE, and A. KUPPERMANN, J. Chem. Phys. **52**, 4516 [1970].
[7] P. D. BURROW and G. J. SCHULZ, Phys. Rev. **187**, 97 [1969].
[8] H. EHRHARDT and F. LINDER, Phys. Rev. Lett. **21**, 419 [1968].
[9] F. LINDER, Abstracts VI-th ICPEAC Cambridge, Mass. 1969, p. 141, MIT Press, Cambridge, Mass., USA.
[10] R. A. ABRAM and A. HERZENBERG, Chem. Phys. Lett. **3**, 187 [1969].
[11] A. V. PHELPS, Rev. Mod. Phys. **40**, 399 [1968]. — R. W. CROMPTON, Advances in Electronics and Electron Physics **27**, 1 [1969], Academic Press, New York.
[12] R. W. CROMPTON, D. K. GIBSON, and A. I. MCINTOSH, Aust. J. Phys. **22**, 715 [1969].
[13] R. W. CROMPTON, D. K. GIBSON, and A. G. ROBERTSON, Phys. Rev. A **2**, 1386 [1970].
[14] R. J. W. HENRY and N. F. LANE, Phys. Rev. **183**, 221 [1969].
[15] E. S. CHANG and A. TEMKIN, Phys. Rev. Lett. **23**, 399 [1969].
[16] S. HARA, J. Phys. Soc. Japan **27**, 1009 [1969].
[17] S. HARA, J. Phys. Soc. Japan **27**, 1592 [1969].
[18] R. J. W. HENRY, Phys. Rev. A **2**, 1349 [1970].
[19] E. S. CHANG, Phys Rev. A **2**, 1403 [1970].
[20] H. EHRHARDT, L. LANGHANS, and F. LINDER, Z. Phys. **214**, 179 [1968].

a multichannel scaler or integrated with a ratemeter and directly plotted on an X-Y-recorder.

Most of the experiments were performed at an energy resolution of 30 – 40 meV which was sufficient to resolve rotational transitions in the energy loss spectrum (see Figs. 1 and 2). Typical beam intensities were $5 \cdot 10^{-10}$ to 10^{-9} A.

The following procedure was adopted to avoid falsification of the ratios of inelastic processes to elastic scattering in the energy loss spectra by transmission effects of the electron optical system. Intensity and shape of the primary beam were controlled by a monitor for energies between 0.3 eV and about 15 eV. Then, the energy dependence of elastic e – He scattering was measured at different angles. As this cross section is quite well known in this energy range from recent investigations [21], the method is well suitable for measuring the transmission properties of the collector system as a function of energy. By applying lens potentials which vary with electron energy a nearly constant transmission of the collector system can be obtained. More details are described in earlier papers [3, 20]. The experimental errors due to transmision effects are expected to be small especially as the processes investigated here lead to only small energy losses of the scattered electrons.

The angular distribution measurements for angles from 20° to 120° have been performed in three independent ways.

(1) The angular dependence has been measured with constant gas pressure in the scattering region, $\sin \vartheta$ being applied as a correction function.

(2) Careful measurements of differential e – He scattering combined with phase shift fits have been performed by ANDRICK and BITSCH [21] recently.. A very narrow gas beam has been used in these measurements so that no correction is needed. These e – He angular distributions have been used to get a correction for the angular dependence measurements in our machine which is working with a rather broad gas beam.

(3) The e – H_2 angular distributions (corrected for rotational excitation contributions) have been measured directly with the narrow gas beam apparatus of Andrick and Bitsch. The results of all methods agree very well. If the angular distributions are normalized at an angle of 90°, the corresponding values at 20° deviate not more than 5% from the average. The agreement is better at all other angles.

Evaluation of Data

Figure 1 shows an energy loss spectrum which has been taken from H_2 with an energy resolution of 30 meV. On the left and right side of the large elastic peak (energy loss 0) contributions can be seen from inelastic and superelastic rotational transitions respectively.

In Fig. 2 the same rotational transitions can be observed in the neighbourhood of the peak for pure vibrational excitation. For the evaluation of these energy loss spectra the following data are needed:

(α) The initial population of rotational states j is given by

$$N(j) \sim (2I+1)\,(2j+1)\,\exp - \frac{B \cdot j(j+1)}{k\,T}. \quad (1)$$

$B = 7.54$ meV is the rotational constant of H_2 in its electronic and vibrational ground state. The nuclear spin I of the H_2-molecule is $I = 0$ for even j, $I = 1$ for odd j. The gas temperature T has been measured with a thermoelement to be $T = 67$ °C. With these data, the following population of rotational states can be calculated from (1): $j = 0$, 11.5%; $j = 1$, 62.8%; $j = 2$, 12.8%; $j = 3$, 11.9%; higher states are populated to less than 1%.

(β) The selection rule $\Delta j = \pm 2$ holds for rotational transitions of a homonuclear diatomic molecule [22]. Transitions with $\Delta j = \pm 4$ are to be expected with much lower intensity [23] and could not be detected in the present experiments.

(γ) The energy levels of the initial and final rotational and vibrational states are calculated from the formula [24]:

$$T = \omega_e(v+\tfrac{1}{2}) - \omega_e x_e (v+\tfrac{1}{2})^2 + B_v\, j(j+1) - D_e\, j^2(j+1)^2 \quad (2)$$

with $B_v = B_e - \alpha_e(v+\tfrac{1}{2})$, $D_e = 4\,B_e^3/\omega_e^2$ and $\omega_e = 4395.2\ \mathrm{cm}^{-1}$, $\omega_e x_e = 117.90\ \mathrm{cm}^{-1}$, $B_e = 60.80\ \mathrm{cm}^{-1}$, $\alpha_e = 2.99\ \mathrm{cm}^{-1}$.

The positions of the expected rotational transitions are indicated by arrows in Figs. 1 and 2.

(δ) The instrumental peak shape has been measured by elastic scattering from helium and argon (dotted line in the upper part of Fig. 1). Special care has been taken to measure the wings. Changes in peak shape when switching from one gas to another can be avoided by using small admixtures of H_2 to the rare gases.

With these data the energy loss spectra can be resolved into separate rotational transition peaks as

[21] D. ANDRICK and A. BITSCH, to be published. The experimental results show good agreement with the calculations of J. CALLAWAY, R. W. LA BAHN, R. T. PU, and W. M. DUXLER, Phys. Rev. **168**, 12 [1968].

[22] K. TAKAYANAGI, Supplement of the Progress of Theoretical Physics **40**, 216 [1967].

[23] N. F. LANE and S. GELTMAN, Phys. Rev. **160**, 52 [1967].

[24] G. HERZBERG, Spectra of Diatomic Molecules, 2. Edition, van Nostrand Company, Princeton, N.J. 1950.

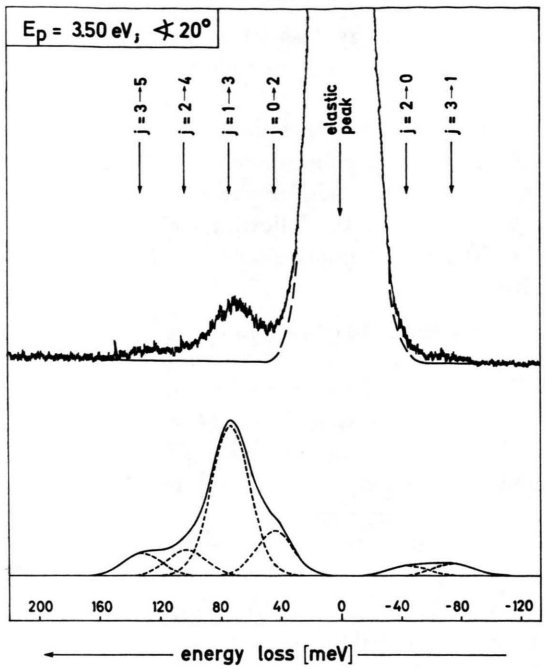

Fig. 1. Upper part: Energy loss spectrum for $e-H_2$ scattering at a collision energy of $E=3.5$ eV and a scattering angle of 20°. Rotational transitions with $\Delta j=\pm 2$ can be observed on both sides of the elastic peak. The dotted line indicates the wings of the elastic peak measured with rare gases (instrumental peak shape). Lower part: The peaks of rotational excitation and deexcitation processes are superimposed with known energy positions, peak shapes, and relative intensities as desribed in the text.

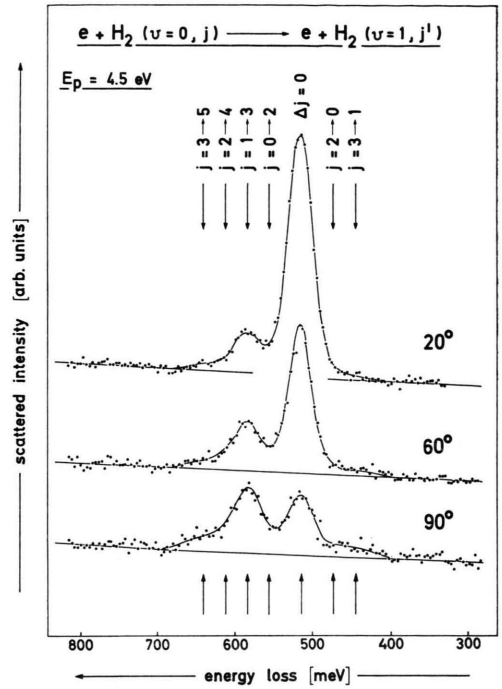

Fig. 2. Energy loss spectra for $e-H_2$ scattering at a collision energy of $E=4.5$ eV and at several scattering angles. The process of pure vibrational excitation ($\Delta j=0$) is accompanied by simultaneous rotational transitions ($\Delta j=\pm 2$). The angular dependence for both processes is completely different.

it is shown in the lower part of Figure 1. The peaks have been superimposed with known energy position and peak shape. The peak heights can be varied until agreement with the measured spectrum is achieved.

The intensity of a rotational transition peak is proportional to $N(j)\cdot\sigma_r(j\to j\pm 2)$, while the elastic and pure vibrational excitation peaks are proportional to $\sum_j N(j)\cdot\sigma_{el}(j\to j)$ and $\sum_j N(j)\cdot\sigma_v(j\to j)$ respectively with $\sum_j N(j)=1$.

In principal, the experiment yields cross sections $\bar{\sigma}_{el}$ and $\bar{\sigma}_v$ which are averaged over all contributing rotational states and depend on the gas temperature, if $\sigma_{el}(j\to j)$ and $\sigma_v(j\to j)$ are different for different j. Calculations on $e-H_2$ scattering indicate that the dependence of $\sigma_{el}(j\to j)$ on j is weak [14, 23], whereas the variation of $\sigma_v(j\to j)$ with j is much stronger [10, 18]. This must be taken into account when experimental and theoretical results for σ_{el} and σ_v are compared.

The cross sections $\sigma_r(j\to j\pm 2)$ for rotational transitions are derived from the energy loss spectra by dividing the peak intensities by the population $N(j)$ of the initial state. The resulting cross sections depend strongly on the initial rotational state j. They can be compared with theoretical predictions of GERJUOY and STEIN [25] for the relative magnitude of rotational excitation cross sections:

$$\sigma_r(j\to j+2)=(k_f/k_i)\cdot\frac{(j+2)(j+1)}{(2j+3)(2j+1)}\,q\,, \quad (3)$$

$$\sigma_r(j\to j-2)=(k_f/k_i)\cdot\frac{j(j-1)}{(2j-1)(2j+1)}\,q\,, \quad (4)$$

where the flux factor k_f/k_i is only important close to threshold and the common factor q determines the absolute magnitude of the cross sections. The relative magnitudes of cross sections resulting from completely different theoretical approaches (close coupling [14, 23], adiabatic theory [15, 17], resonance model [10]) are in excellent agreement with these formulae which were obtained in Born approximation. In all cases, where the ratios of cross sections were extracted from the measured energy loss spectra as

[25] E. GERJUOY and S. STEIN, Phys. Rev. **97**, 1671 [1955].

shown in Fig. 1, good agreement was found with formula (3) and (4). Therefore, in the following only the process $j=1 \rightarrow 3$ was evaluated. The cross sections for all other processes including superelastic collisions are then given by formula (3) and (4).

The procedure of evaluating the data is now as follows. From the energy loss spectra which are taken at angles between 20° and 120° the ratios of all inelastic processes to elastic scattering can be measured. From these ratios together with the angular dependence of elastic scattering from H_2 which has been measured in a separate experiment, the angular distributions for all processes are derived. In order to put all cross secions on an absolute scale one proceeds in the following way. The differential cross sections are integrated over the total solid angle 4π. It is necessary to extrapolate the weighted cross sections $\sigma(\vartheta) \cdot \sin\vartheta$ to 0° and 180°. In most cases this is possible without serious errors. The sum of all integral cross sections at each energy is normalized to the absolute total cross section of GOLDEN, BANDEL, and SALERNO [26]. This leads to absolute units for all integral and differential cross sections of this work.

Discussion of Errors

The experimental errors of the data depend on the form in which the data shall be compared with theory. For instance, any angular distribution has smaller errors in arbitrary units than in absolute units. Ratios of angular distributions are easier to extract from the measurements than angular distributions themselves. Therefore, an analysis of experimental errors will be given here. The discussion of errors follows the process of evaluating the data.

I. The accuracy of the ratios of cross sections, which are the primary result of the measurements, depends on the processes considered and on energy and angle. Estimated errors are listed in the following table:

Energy [eV]	σ_r/σ_{el} [%]	σ_{rv}/σ_{el} [%]	σ_v/σ_{el} [%]	σ_v/σ_{rv} [%]
0.3–1	30–10	—	—	—
1.5	5	20	10–20	10–20
2.5–6	<5	5	≦5	5–10
>6	5	10	5–10	10–15

The main contribution comes frome the statistical error of the weak inelastic signals which are often in the order of 1 c/sec or lower. Smaller contributions result from the unfolding procedure, from the determination of the values $N(j)$, and from transmission effects of the collector system. The error in σ_r/σ_{el} is increased from 10% to 30% for energies from 1 eV to 0.3 eV because rapidly decreasing inelastic signals have to be detected close to the wings of the large elastic peak. This was the reason why the measurements were not continued to energies below 0.3 eV. For σ_v/σ_{el} and σ_v/σ_{rv} the errors depend on the scattering angle and increase from small to large angles with decreasing intensity. The errors of σ_v/σ_{rv} are somewhat smaller than the combined errors of σ_v/σ_{el} and σ_{rv}/σ_{el}.

II. Going from the ratios of angular distributions to the angular distributions themselves an additional uncertainty is introduced by the error of σ_{el}. As already mentioned above, the error must be estimated to 5% for small angles if the angular distribution is fixed at 90°.

III. The extrapolation of $\sigma(\vartheta) \cdot \sin\vartheta$ to 0° and 180° causes an error for the integrated cross sections. In all cases where the theoretical angular distributions agree fairly well with experiment and consequently can be used as guide for the extrapolation, i. e. for σ_{el}, σ_r, and σ_{rv}, the error for the integral introduced by extrapolation should be smaller than 5%. The corresponding error of the integrated cross section for vibrational excitation is estimated to about 10% and could even be larger for the higher energies where pronounced backward scattering introduces higher uncertainty.

IV. No additional error is introduced by the summation of all integral cross sections to the total cross section, since contributions from processes which have not been measured in this work (vibrational excitation [3] to $v \geqq 2$, dissociation [5, 27] of H_2, dissociative attachment [28–30]) are very small. The error in the sum of all integral cross sections is dominated by the error of the elastic cross section (σ_{el} gives 90% of the total cross section) and is estimated to about 5%.

V. The accuracy of the absolute total cross sections measured by GOLDEN, BANDEL, and SALERNO [26] is estimated to about 3% by the authors. The agreement with the older measurements of RAMSAUER and KOLLATH [31] is better than 5% except for energies below 1 eV and around 10 eV. Our absolute scale has been normalized to the cross sections of Ref. [26]. The use of other data would lead to a renormalization of all cross sections of this work.

[26] D. E. GOLDEN, H. W. BANDEL, and J. A. SALERNO, Phys. Rev. **146**, 40 [1966].
[27] S. B. J. CORRIGAN, J. Chem. Phys. **43**, 4381 [1965].
[28] G. J. SCHULZ, Phys. Rev. **113**, 816 [1959].
[29] D. RAPP, T. E. SHARP, and D. D. BRIGLIA, Phys. Rev. Lett. **14**, 533 [1965].
[30] G. J. SCHULZ and R. K. ASUNDI, Phys. Rev. Lett. **15**, 946 [1965].
[31] C. RAMSAUER and R. KOLLATH, Ann. Phys. **4**, 91 [1930]; **12**, 529 [1932].

Results and Discussion

a) General Survey

Figure 3 shows a selection of H_2- and H_2^--states which are of importance for the processes investigated here. The very short-lived H_2^--state with $^2\Sigma_u^+$-configuration around 3 eV leads to a very broad shape resonance in the cross sections [1, 3, 9]. The electron is captured in the field of the ground state of the H_2-molecule by the centrifugal barrier. Therefore, a shape resonance (or open channel resonance) is always connected with partial waves $l>0$.

Another type of resonance is caused by the H_2^--state of $^2\Sigma_g^+$-configuration at 11.3 eV. In this case the electron is trapped in the potential of one (or both) of the excited states of the H_2-molecule shown in the figure [32]. This type of resonance is called a Feshbach-resonance or closed channel resonance. Recent experimental investigations [4, 5] have shown that there are much more Feshbach resonant states in this energy region. But it is predominantly the $^2\Sigma_g^+$ resonant state shown in Fig. 3 which is responsible for the resonance structure in the cross sections for rotational and vibrational excitation of H_2.

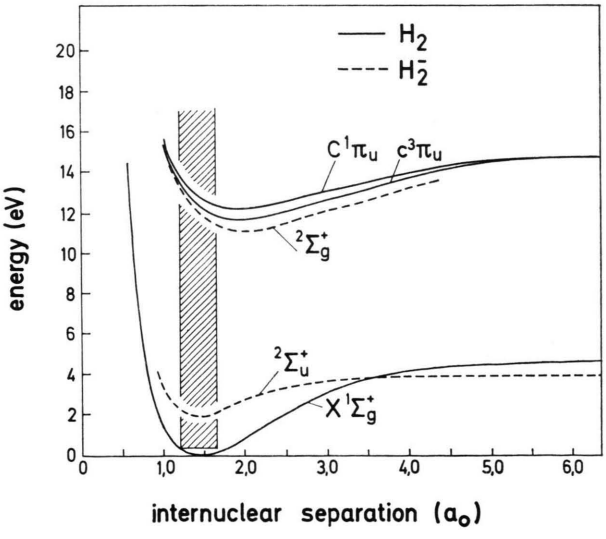

Fig. 3. Potential energy curves for some H_2^- resonant states (dotted lines) and some H_2 states (full lines), which are of importance for the processes investigated in this paper.

It seems reasonable that $^2\Sigma_g^+$ is a frequently occurring configuration among the Feshbach resonances of H_2, because the resonant state is formed as lowest bound state in the potential of the excited molecule, corresponding to an S-state in the case of an atom. Resonant states with other configurations would have higher energy and may be expected in most cases as shape resonances in the inelastic channel for excitation of the parent state [20]. Since for the processes investigated here the initial and final state of the H_2-molecule is the $X\,^1\Sigma_g^+$-ground state, the formation and the decay of an H_2^--$^2\Sigma_g^+$-Feshbach resonance predominantly occurs by s-wave scattering. This is contrary to the case of a shape resonance.

The experimental results of this work are discussed in terms of resonance scattering superimposed on a background of direct scattering. The resonance model is very well suited to bring out simple physical features of the scattering processes. However, it is necessary to describe briefly the other theoretical approaches, the results of which are compared with the present measurements.

The resonance model has been successfully applied to electron molecule scattering [33–35]. Among the numerous electron molecule resonances the $^2\Sigma_u^+$-shape resonance at 3 eV in $e-H_2$ scattering is an interesting example because of its very short lifetime. The prediction of a dominant $p\sigma$-wave for this case was confirmed by experiment [3]. However, the agreement was only qualitative. The separation of vibrational excitation into pure vibrational and simultaneous rotational and vibrational excitation gave the same findings [9, 10]. The conclusion is that the resonance scattering concept is very useful as a simple model, but must be extended if the scattering processes are to be described in a quantitative way.

A different approach including all participating partial waves is the rotational close coupling method which takes full account of the molecular rotation. The $e-H_2$ problem, i. e. elastic scattering and rotational excitation [23, 24] and recently vibrational excitation [18] has been successfully treated by this method up to energies of about 10 eV. Agreement be-

[32] J. ELIZIER, H. S. TAYLOR, and J. K. WILLIAMS, J. Chem. Phys. **47**, 2165 [1967].
[33] J. N. BARDSLEY and F. MANDL, Reports on Progress in Phys. **31**, 471 [1968].
[34] F. H. READ, J. Phys. B (Proc. Phys. Soc., Ser. 2) **1**, 893 [1968].
[35] T. F. O'MALLEY and H. S. TAYLOR, Phys. Rev. **176**, 207 [1968].

tween theory and experiment is generally good, but the physical interpretation of the results is not as easy as in the case of the resonance model.

The third method, the so-called adiabatic theory [15, 17] makes use of the fact that the time needed for the scattering process is usually very small compared to the period of molecular rotation. As a first step, the scattering amplitude $f(\Omega, \Omega')$ is evaluated for a fixed orientation of the molecule (Ω = orientation of the molecular axis, Ω' = scattering angle of the scattered electron, both relative to the direction of the incoming electron). Then, the cross section for a rotational transition $j \to j'$ is represented by the formula

$$\sigma(j \to j') = k_{j'}/k_j \frac{1}{2j+1} \sum_m \sum_{m'} |\langle Y_{j'm'}(\Omega) | f(\Omega, \Omega') | Y_{jm}(\Omega) \rangle|^2, \quad (5)$$

where the cross sections for individual transitions $(j, m) \to (j', m')$ have been summed over final substates m' and averaged over initial substates m. $k_{j'}/k_j$ is a flux factor. For $j = j'$, formula (5) describes pure elastic scattering without change of the rotational state j.

Both the close-coupling and the adiabatic theory do not anticipate the existence of a resonance at 3 eV in $e - H_2$ scattering. However, though equally containing all partial waves both approaches find that all processes are strongly dominated by p-wave scattering in accordance with the resonance model. It seems not worthwhile to discuss whether the resonance exists or does not. The very broad shape resonance is certainly situated on the boundary between direct and resonance scattering. On the other hand, a good calculation of direct scattering must yield an open channel resonance like the 3 eV-resonance in $e - H_2$ scattering. This means, that, strictly speaking, a boundary between direct scattering and resonance scattering does not exist.

We prefer to retain the resonance concept in this case and interprete the scattering processes in the energy region around 3 eV as superposition of resonance and direct scattering. The fact that the phase shift of the p-wave does not increase by π over the resonance region must then be explained by the variation of the phase shift of direct scattering in the same energy region, which seems plausible because of the large width of the resonance.

b) Direct Scattering and Excitation by a Shape Resonance

Elastic scattering is a special case of Eq. (5) and therefore an important process in connection with rotational excitation. Figure 4 shows measured angular distributions for pure elastic scattering compared with different theories [14, 16]. In arbitrary units the experimental errors are only due to point (II) of the error discussion. All curves are arbitrarily normalized to each other at 90°. At 10 eV, experimental results of TRAJMAR et al. [6] are also shown, which have been normalized to our measurements around 70°. The agreement would still be better, if the results of TRAJMAR et al. [6] would be corrected for rotational excitation contribution which are not resolved in these measurements.

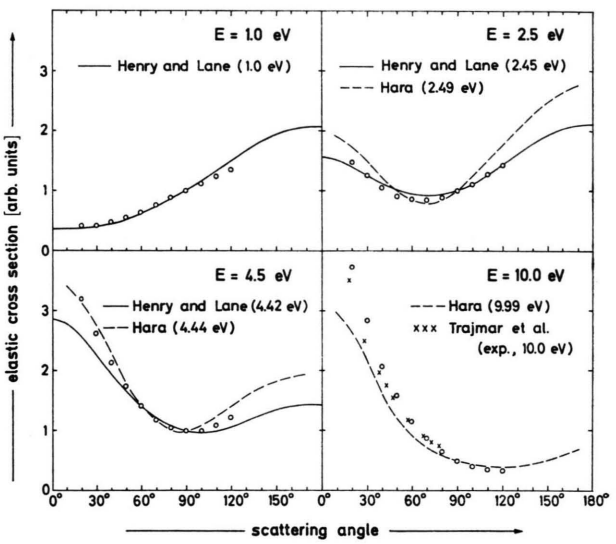

Fig. 4. Measured angular distributions for pure elastic scattering from H_2 at different collision energies (open circles) compared with theoretical results of HENRY and LANE [14] and of HARA [16, 17] and with experimental results of TRAJMAR et al [6]. All curves are arbitrarily normalized at 90°. The measurements of Trajmar et al. are normalized to the results of this work around 70°. The results of Hara and of Trajmar et al. include contributions from rotational excitation processes.

When comparing our results with theory one has to consider that the adiabatic theory of Hara also contains rotational excitation contributions [17], while the calculations of Henry and Lane are for pure elastic scattering. However, one can easily see

from our results on rotational excitation that this cannot be responsible for the differences between both calculations. It seems that the calculations of Henry and Lane agree very well at low energies, while at higher energies the calculations of Hara become better. This is confirmed by comparison of both calculations with the measured integral cross section for rotational excitation (Fig. 7). It is interesting to notice that at 4.5 eV agreement and disagreement between experiment and both calculations behave in a very similar way for both differential elastic (Fig. 4) and rotational excitation cross section (Fig. 5).

The rapid and drastic variation of the elastic angular distributions with energy indicates large contributions from direct scattering. The calculations [16] show that s-wave and p-wave scattering give comparable contributions and that the ratio varies quite rapidly with energy.

Figure 5 presents angular distributions in arbitrary units for the inelastic processes in the energy range from 2.5 eV to 10.8 eV. As far as possible the experimental results are compared with theory. The solid lines are the predictions of the pure resonance model of ABRAM and HERZENBERG [10]. The results of the other calculations (HENRY and LANE [14], CHANG and TEMKIN [15], HARA [17], HENRY [18]) are indicated in the figure.

The comparison between experiment and theory depends on normalization to some extent. First of all, the ratios σ_v/σ_{rv} can be directly compared with each other and are free from normalization problems. Then, either σ_v or σ_{rv} could be normalized to theory. Since there are physical reasons that σ_r and σ_{rv} are expected to agree quite well with theory, we have arbitrarily normalized all determinations of σ_r and σ_{rv} to each other around 90°. σ_v is then no longer freely adjustable. It is a consequence of

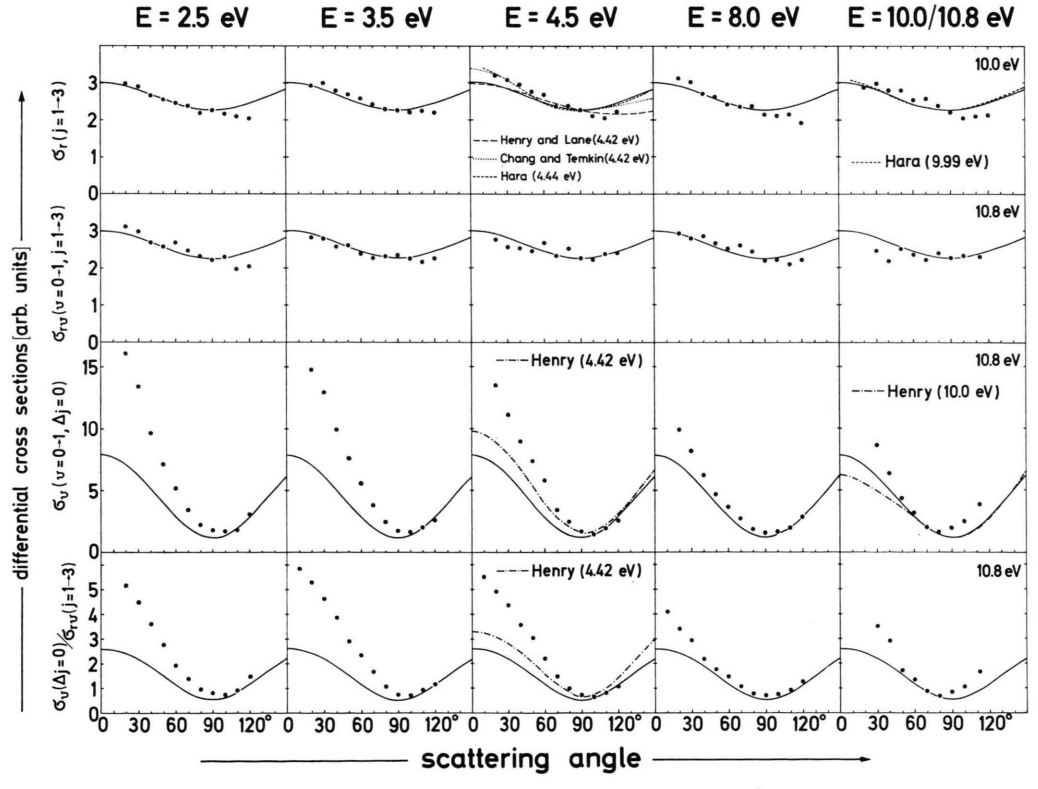

Fig. 5. Measured angular distributions for the processes σ_r ($j=1\rightarrow 3$), σ_{rv} ($v=0\rightarrow 1$; $j=1\rightarrow 3$), σ_v ($v=0\rightarrow 1$; $\Delta j=0$) and for the ratios $\sigma_v(\Delta j=0)/\sigma_{vr}(j=1\rightarrow 3)$ at different collision energies (full points). The results are compared in arbitrary units with different theories: ABRAM and HERZENBERG [10] (full lines), HENRY and LANE [14], CHANG and TEMKIN [15], HARA [17], HENRY [18]. The normalization problem and the question of temperature dependence of the angular distributions are discussed in the text.

this procedure that the discrepancies in σ_v are emphasized, whereas the agreement in σ_r and σ_{rv} becomes good. However, we think that this choice of normalization has physical relevance, as is discussed below. As in the case of elastic scattering the comparison has been carried out in arbitrary units because of the smaller experimental errors which only come from points (I) and (II) of the error discussion. – It should be mentioned that at 10.8 eV both theoretical curves for σ_v are arbitrarily normalized to each other at 90°, while at 4.5 eV the dotted line for $\sigma_v(\vartheta)$ is derived from Henry's rations $\sigma_v/\sigma_{rv}(\vartheta)$ by assuming that the angular distribution $\sigma_r(\vartheta)$ from Henry and Lane is identical with $\sigma_{rv}(\vartheta)$ at the same energy.

The pure vibrational excitation cross section is an average over all contributing rotational states:

$$\bar{\sigma}_v(\vartheta) = \sum_j N(j) \cdot \sigma_v(j \to j; \vartheta).$$

Since the individual cross sections $\sigma_v(j \to j; \vartheta)$ depend quite strongly on j [10, 18], a temperature dependence of $\bar{\sigma}_v(\vartheta)$ has to be expected. If from the data of Abram and Herzenberg the angular distribution is calculated for a temperature $T = 67$ °C at which the experiments have been performed, the resulting angular dependence $\bar{\sigma}_v(\vartheta) = 1.2 + 6.6 \cdot \cos^2\vartheta$ is practically identical with that for $T = 20$ °C. That means that in spite of the strong dependence of $\sigma_v(j \to j; \vartheta)$ on j the averaged cross section $\bar{\sigma}_v(\vartheta)$ seems to be very insensitive to temperature changes. As far as can be seen from the results of Henry the same is true for the close coupling results which are very similar to the predictions of the resonance model in this case.

The resonance model of Abram and Herzenberg assumes pure resonance scattering for all processes of Fig. 5, the scattering electron being a σ_u-electron. The first approximation to a σ_u-electron is a pσ-wave, which is the only partial wave that has been retained in the calculations of Abram and Herzenberg. The assumptions lead to an angular distribution for each process which is constant over the whole energy range. The fact that the measured angular distributions do not vary with energy as rapidly as in the case of elastic scattering can be taken as an indication that resonance scattering is much more dominant for the inelastic processes. Deviations from this simple model indicate the participation of other partial waves, which can be either from direct scattering or from higher terms of the resonance scattering amplitude. Since, however, the next resonance term is the fσ-wave, which is somewhat unlikely to be involved at these low energies, it seems to be more probable that the deviations come from direct scattering contributions. A further indication for this conclusion is that higher terms of resonance scattering cannot disturb the symmetry around 90°.

The angular distributions for the rotational excitation processes σ_r and σ_{rv} can be assumed to be equal. The conclusion that the p-wave is the dominant partial wave for these processes is independent of the theoretical approach. Without using the resonance model one sees that pure s-wave scattering (i. e. s → s) does not contribute, while higher partial waves than $l = 1$ are more or less outside the range of interaction. This is the reason for the normalization procedure described above.

The angular distributions for pure vibrational excitation and hence the ratios σ_v/σ_{rv} show a clear variation with energy. They are steeper at low energies, and the minimum is shifted from 100° to 80° while going from low to higher energies. The asymmetry around 90° indicates that it is not a higher partial wave of resonance scattering (i. e. fσ-wave) which can explain the experimental results. It seems reasonable that a relatively large direct scattering amplitude must be considered for the process of pure vibrational excitation. The main contribution should come from the s-wave. The recent close coupling calculations of HENRY [18] yield a strongly dominating p-wave also for this process. The comparison in Fig. 5 shows that the calculations underestimate the contributions from other partial waves. However, the theory seems to have the right tendency, because the experimental finding that forward scattering dominates at lower energies and that the opposite behaviour results for higher energies is also indicated in the theoretical curves though less pronounced.

In conclusion one can say that the relative contribution of direct scattering seems to decrease when going from elastic scattering to pure vibrational excitation, while the rotational excitation processes are quite well described by pure p-wave scattering independently of the theoretical approach. TRAJMAR et al. [6] have carried out an experimental and theoretical investigation of vibrational excitation of H_2 to $v = 1$, 2, and 3 (without resolving rotations). They make an attempt to separate the cross sections for

the processes into direct and resonance scattering contributions, and they find that for the energy range of our Fig. 4 and 5 the resonance contribution becomes more and more dominant with increasing vibrational quantum number of the final state. These findings combined with our results discussed above support the conclusion that for the energy range up to about 10 eV the processes of elastic scattering ($v=0$) and vibrational excitation ($v=1$, 2, 3) of H_2 can be interpreted in terms of superposition of direct and resonance scattering with decreasing importance of the direct scattering amplitude.

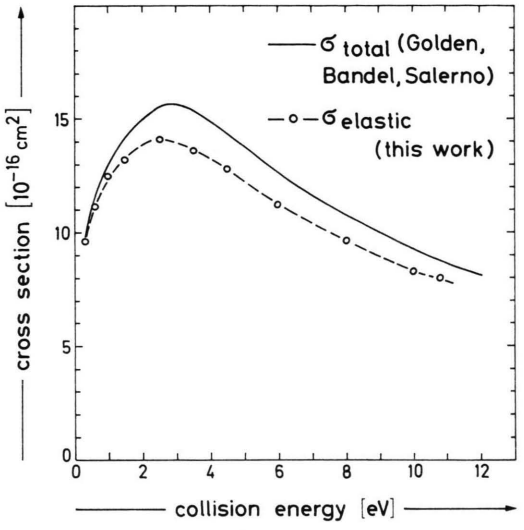

Fig. 6. Integral cross section in absolute units for pure elastic scattering from H_2 as a function of collision energy determined from the measurements of this work. For comparison the total cross section of GOLDEN, BANDEL, and SALERNO [26] is shown to which all measurements of this work have been normalized. The difference between σ_{total} and $\sigma_{elastic}$ represents the sum of all inelastic cross sections.

Figure 6 shows the integral elastic cross section $\bar{\sigma}_{el}=\sum_j N(j)\cdot\sigma_{el}(j\to j)$ of this work together with the total cross section determined by GOLDEN, BANDEL, and SALERNO [26]. As an average over all contributing rotational states j the elastic cross section is expected to depend on temperature. However, this temperature dependence seems to be very weak [14, 23]. The cross section $\sigma=\sum_{j'}\sigma(j\to j')$, which is the sum of the cross sections for elastic scattering and for rotational excitation, does not depend on j as has been shown in the adiabatic theory [15–17].

Figure 7 presents the integral rotational excitation cross section $\sigma_r(j=1\to 3)$ in absolute units compared with different calculations which have already been discussed together with Figs. 4 and 5. The experimental errors come from all sources listed in the error discussion. If the individual errors are combined according to the error law of Gauss, the uncertainty of the experimental points should not exceed 10% for energies around 4 eV, while it becomes as much as 30% for the lowest energy measured.

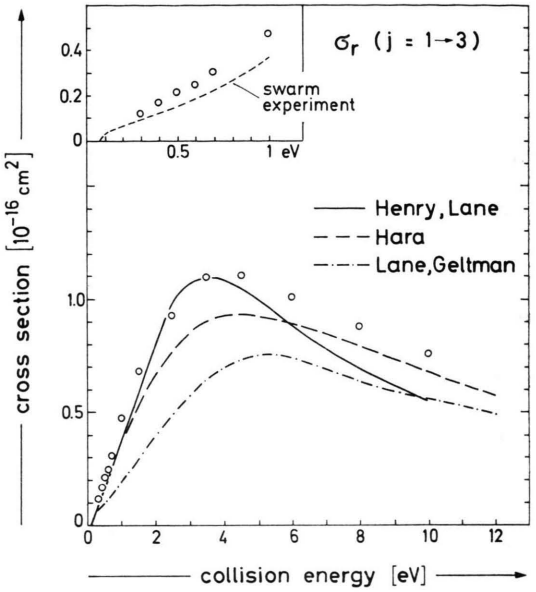

Fig. 7. Measured integral cross section σ_r ($j=1\to 3$) in absolute units (open circles) for pure rotational excitation $j=1\to 3$ of the H_2 molecule as a function of collision energy. The experimental results are compared with the calculations of HENRY and LANE [14], of HARA [17], and of LANE and GELTMAN [23]. The insert with expanded energy scale compares the results of the present beam experiment with the results of a swarm experiment of CROMPTON et al. [12]. The swarm data have been transformed from σ_r ($j=0\to 2$) to σ_r ($j=1\to 3$) as described in the text.

The insert of Fig. 7 with an expanded energy scale shows the low energy region where our results have been compared with the results of the swarm experiments of CROMPTON et al. [12]. The swarm data have been transformed from σ_r ($j=0\to 2$) to σ_r ($j=1\to 3$) by the formula

$$\sigma_r(j=1\to 3)=\tfrac{3}{5}\cdot\sigma_r(j=0\to 2)\left(\frac{E-74\text{ meV}}{E-44\text{ meV}}\right)^{1/2} \quad (6)$$

which is a consequence of Equation (3). In this way, one gets a certain range of overlap between swarm experiment and beam experiment. Our results are somewhat higher, but at present the errors of both experiments are such that both methods agree with-

in their error bars. The error of the beam experiment increases from about 15% at 1 eV to 30% at 0.3 eV, while the error of the swarm experiment grows rapidly from 5% at 0.3 eV to 30% at 0.5 eV. From 0.5 eV to 1 eV the cross section of Crompton et al. has been extrapolated with the aid of the theoretical cross section on Henry and Lane. These findings express the complementary character of both methods in the low energy region.

The integral cross sections for pure vibrational excitation σ_v ($v=0\rightarrow 1$; $\Delta j=0$) and for simultaneous rotational and vibrational excitation σ_{rv} ($v=0\rightarrow 1$; $j=1\rightarrow 3$) are presented in absolute units in Fig. 8 and are compared with the recent close coupling calculations of HENRY [18]. The agreement in the absolute magnitude of the cross sections is poor, while the ratios of both cross sections are much better in agreement. The p-wave contribution seems to be overestimated in the calculations. The experimental error is composed in the same way as in the case of Fig. 7 and is estimated to 10% near the maxima of the curves, while it increases to about 20% for the lowest and highest energies measured.

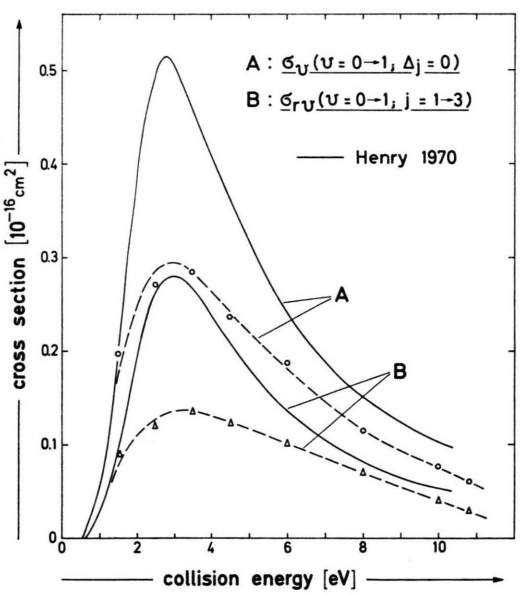

Fig. 8. Measured integral cross section σ_v ($v=0\rightarrow 1$; $\Delta j=0$) for pure vibrational excitation $v=0\rightarrow 1$; $\Delta j=0$ (open circles) and σ_{rv} ($v=0\rightarrow 1$; $j=1\rightarrow 3$) for simultaneous rotational-vibrational excitation $v=0\rightarrow 1$; $j=1\rightarrow 3$ (triangles) of H_2 as a function of collision energy. The experimental results are presented in absolute units and compared with recent calculations of HENRY [18]. The dotted lines represent an arbitrary interpolation between the measured points.

The investigation of the temperature dependence of the pure vibrational excitation cross section gives the same result as for the differential cross section. It follows from both theoretical approaches [10, 18] that the temperature dependence of $\bar{\sigma}_v=\sum_j N(j)\cdot\sigma_v(j\rightarrow j)$ is very weak in spite of a strong dependence of $\sigma_v(j\rightarrow j)$ on j.

From the data of Fig. 8 one can calculate the total vibrational excitation cross section σ_{v+rv} by the equation

$$\begin{aligned}\sigma_{v+rv}&=\sum_j N(j)\cdot[\sigma_v(j\rightarrow j)+\sigma_{rv}(j\rightarrow j+2)\\&\quad+\sigma_{rv}(j\rightarrow j-2)]\\&=\bar{\sigma}_v+1.12\,\sigma_{rv}(j=1\rightarrow 3)\end{aligned}\qquad(7)$$

which follows by using the distribution $N(j)$ of rotational states at $T=67^\circ$ and with the aid of Eqs. (3) and (4) for the relative rotational excitation cross sections. The resulting cross section σ_{v+rv} can be compared with an earlier direct determination [3] of the total vibrational excitation cross section $v=0\rightarrow 1$. Both results agree within their error limits.

A recent experimental study of σ_{v+rv} near threshold performed by CROMPTON et al. [12, 13] in swarm experiments completes the information on this cross section towards the low energy region. The authors discuss in detail the comparability of both determinations, which is a nontrivial problem [13], and find a cross section which is about 30% lower around 1 eV than in Ref. [3]. To higher collision energies up to 80 eV the process of vibrational excitation (σ_{v+rv}) has been investigated by TRAJMAR et al. [6]. In the region of overlap with the measurements of Ref. [3] the agreement is generally good.

In Tables 1 to 4 the differential cross sections for all processes and most of the collision energies investigated in this work have been listed in absolute units. The experimental errors are larger due to the absolute scale than in the case where the numbers are used as angular distributions in arbitrary units as in Fig. 4 and 5. The errors for the differential elastic cross sections (Table 1) come from points (II), (IV), and (V) of the error discussion. The inelastic cross sections of Tables 2 to 4 are directly derived from the ratios $\sigma_{inel}/\sigma_{el}(\vartheta)$. The errors are therefore composed of the errors of the ratios [point (I) of the error discussion] and those of $\sigma_{el}(\vartheta)$.

Table 1. Differential cross sections in absolute units [10^{-16} cm^2/ster] for elastic e$-$H$_2$ scattering.

Scatt. angle [°]	Collision energy [eV]									
	0.6	1.0	1.5	2.5	3.5	4.5	6.0	8.0	10.0	10.8
20	0.39	0.46	0.61	1.35	1.86	2.24	2.49	2.60	2.61	2.64
30	0.42	0.46	0.57	1.15	1.57	1.83	2.02	2.10	1.99	2.05
40	0.47	0.49	0.57	0.97	1.29	1.49	1.61	1.61	1.44	1.52
50	0.53	0.55	0.60	0.84	1.09	1.22	1.28	1.25	1.11	1.12
60	0.61	0.63	0.66	0.79	0.92	0.97	1.00	0.96	0.80	0.83
70	0.72	0.75	0.75	0.78	0.82	0.81	0.80	0.73	0.61	0.59
80	0.82	0.87	0.89	0.82	0.78	0.73	0.66	0.57	0.45	0.44
90	0.93	0.99	1.03	0.92	0.79	0.70	0.57	0.46	0.35	0.34
100	1.01	1.09	1.17	1.02	0.84	0.70	0.52	0.40	0.28	0.27
110	1.08	1.19	1.35	1.18	0.93	0.74	0.53	0.37	0.25	0.23
120	1.14	1.28	1.44	1.33	1.03	0.84	0.57	0.35	0.23	0.20

Table 2. Differential cross sections in absolute units [10^{-17} cm^2/ster] for rotational excitation of H$_2$; σ_r ($j=1\rightarrow3$, $\Delta v=0$).

Scatt. angle [°]	Collision energy [eV]						
	1.5	2.5	3.5	4.5	6.0	8.0	10.0
20	0.60	0.97	1.06	1.17	1.11	0.91	0.73
30	0.57	0.93	1.10	1.13	1.08	0.93	0.76
40	0.56	0.86	1.02	1.09	0.99	0.82	0.70
50	0.53	0.83	0.97	1.02	0.88	0.79	0.70
60	0.54	0.80	0.94	0.97	0.85	0.74	0.64
70	0.52	0.77	0.87	0.85	0.77	0.72	0.65
80	0.58	0.71	0.84	0.87	0.75	0.72	0.61
90	0.59	0.73	0.81	0.84	0.79	0.66	0.56
100	0.53	0.70	0.80	0.78	0.73	0.65	0.51
110	0.53	0.67	0.80	0.74	0.71	0.65	0.54
120	0.52	0.66	0.79	0.80	0.73	0.58	0.55

Table 3. Differential cross sections in absolute units [10^{-18} cm^2/ster] for vibrational excitation of H$_2$; $\sigma_v(v=0\rightarrow1, \Delta j=0)$.

Scatt. angle [°]	Collision energy [eV]						
	1.5	2.5	3.5	4.5	6.0	8.0	10.8
20	3.80	6.50	6.60	5.38	4.35	2.33	—
30	2.96	5.40	5.73	4.45	3.35	1.91	0.86
40	2.22	3.93	4.40	3.58	2.66	1.45	0.60
50	1.60	2.90	3.32	2.92	1.83	1.09	0.43
60	1.03	2.10	2.50	2.28	1.33	0.85	0.31
70	1.08	1.37	1.67	1.34	0.88	0.63	0.19
80	0.68	0.91	1.10	0.98	0.75	0.42	0.16
90	0.67	0.73	0.78	0.65	0.52	0.36	0.19
100	0.68	0.70	0.72	0.56	0.61	0.39	0.24
110	1.02	0.73	0.89	0.75	0.65	0.46	0.39
120	1.34	1.24	1.17	1.01	0.91	0.65	(*113°*)

c) Direct Scattering and Excitation by a Feshbach-Resonance

The energy range above 11 eV is characterized by the superposition of direct scattering and several Feshbach-resonances. It is predominantly one of these Feshbach-resonances which is responsible for

Table 4. Differential cross sections in absolute units [10^{-18} cm^2/ster] for simultaneous rotational and vibrational excitation of H$_2$; σ_{rv} ($j=1\rightarrow3$, $v=0\rightarrow1$).

Scatt. angle [°]	Collision energy [eV]						
	1.5	2.5	3.5	4.5	6.0	8.0	10.8
20	0.66	1.24	1.25	1.11	0.93	0.69	—
30	0.59	1.20	1.24	1.02	0.89	0.65	0.25
40	0.61	1.08	1.13	1.01	0.84	0.67	0.23
50	0.66	1.04	1.14	0.97	0.78	0.62	0.25
60	0.60	1.08	1.05	1.04	0.78	0.59	0.23
70	0.79	0.99	1.00	0.90	0.71	0.60	0.22
80	0.81	0.94	1.02	1.00	0.82	0.57	0.23
90	0.70	0.89	1.03	0.91	0.76	0.52	0.23
100	0.86	0.92	1.00	0.89	0.80	0.53	0.23
110	0.66	0.80	0.95	0.94	0.77	0.50	0.22
120	0.86	0.81	1.00	0.94	0.75	0.52	(*113°*)

the structures in the excitation functions of the electronic ground state [4, 5]. Figure 9 shows some examples. The two upper curves are differential cross sections for excitation of $v=1$ at scattering angles of 40° and 90°, the lower curve is the excitation function of $v=4$ at 100°, in all cases without resolving rotational transitions. These curves have been taken from Ref. [5] because of their importance for the following experiments of this work. In the exit channel $v=1$ direct scattering and resonance scattering are superimposed with comparable amplitudes, while in channel $v=4$ one has nearly pure resonance scattering and practically no excitation outside the resonances. The structures in each channel belong to different vibrational levels of one H_2^--state which has been shown to have $^2\Sigma_g^+$-configuration [5].

The absolute scales in Fig. 9 are related to the direct scattering cross section σ_{v+rv} outside the resonances. A re-examination of the absolute scales

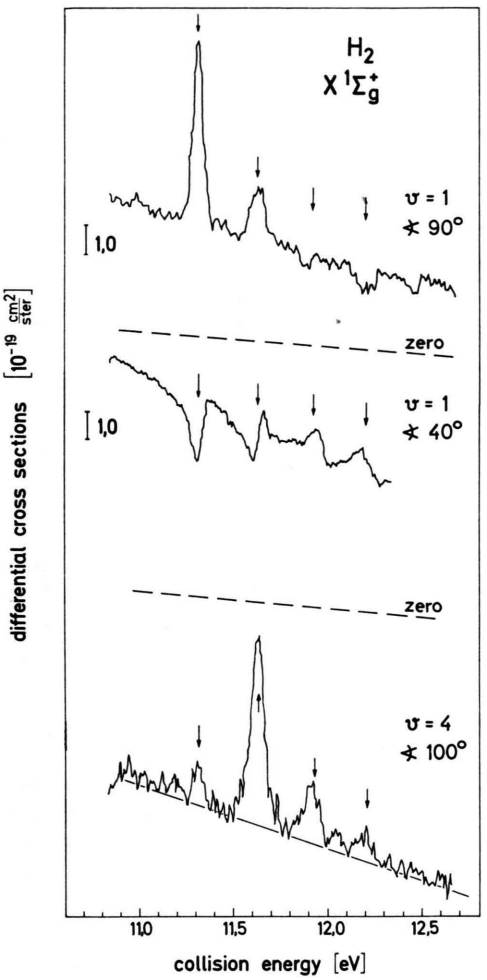

Fig. 9. Measured differential cross sections for vibrational excitation of H_2 as a function of collision energy (without resolving rotations) [5]. Exit channels and scattering angles are indicated in the figure. The dashed zero lines show the variation of the unphysical background with energy. The bars to the left of the curves represent the scaling factors in units of $1 \cdot 10^{-19}$ cm²/ster. The structures in the curves indicated by small arrows are due to the vibrational levels of the H_2^- Feshbach state shown in Figure 3.

for the electronic ground state measurements of Ref. [5] showed that in some cases the differential cross sections need corrections which are mainly due to errors in the former angular distribution measurements. The absolute scales of Fig. 9 have been corrected and are consistent with the results of Tables 3 and 4 of this work. The effect of these corrections on the integrated cros sections of Ref. [5] is small.

The results of Fig. 9 outside the resonances can be compared with measurements of TRAJMAR et al. [6] performed at collision energies of 10 eV and 13.6 eV. If our curves for channel $v = 1$ are extrapolated to these energies, very good agreement with the results of Trajmar et al. is found.

The question, which is of physical interest for the investigations of this paper, is to compare the mechanisms of direct and Feshbach-resonance scattering concerning rotational and vibrational excitation. For a collision energy of 11.62 eV and for the exit channel $v = 4$ one has pure resonance scattering. At an energy of 10.8 eV one is well outside the Feshbach-resonances. On the other hand it is reasonable to assume that contributions from the shape resonance at low energies can be neglected at this energy in channel $v = 1$, which is supported by theoretical considerations of TRAJMAR et al. [6]. That means that one can compare the direct excitation mechanism ($E = 10.8$ eV; $v = 1$) with the excitation mechanism by a Fershbach-resonance ($E = 11.62$ eV; $v = 4$) at nearly the same energy. This has been done in Fig. 10, where for both cases energy loss spectra for three different angles are shown.

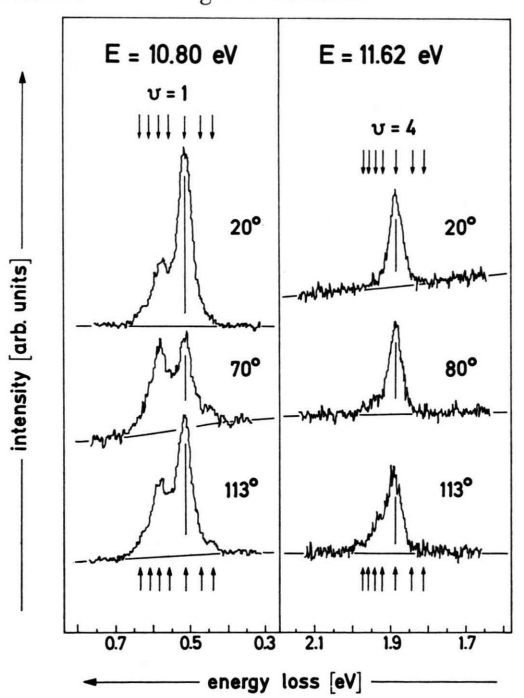

Fig. 10. Energy loss spectra; a) for the direct excitation process ($E = 10.80$ eV; exit channel $v = 1$; left side) and b) for the Feshbach-resonance excitation process ($E = 11.62$ eV; exit channel $v = 4$; right side) at several scattering angles. For selection of collision energies and exit channels see Figure 9. The arrows indicate the positions of the expected rotational transitions as in Figure 2. The rotational excitation contributions are completely different for both scattering processes.

The arrows indicate the positions of the same rotational transitions as in Fig. 2. The striking feature of Fig. 10 is that the rotational excitation contributions are completely different in both cases. The reason is given by the distinct participation of the partial waves in both scattering processes. While the process of direct scattering contains several partial waves which can cause rotational transitions of the molecule, the resonance process in dominated by pure s-wave scattering. The formation of the $H_2^- {}^2\Sigma_g^+$-state and its decay into the electronic ground state $X\,{}^1\Sigma_g^+$ $(v=4)$ of H_2 occurs by a σ_g-electron which can be represented by an s-wave in a first approximation. The weak rotational transitions, however, which can be observed besides the peak for pure vibrational excitation to $v=4$ indicate that other partial waves are also involved to some extent. These can come either from higher terms of the resonance scattering amplitude (i. e. mainly d-wave including $s \rightarrow d$ and $d \rightarrow s$ contributions) or from a small amount of direct scattering superimposed on resonance scattering. In the latter case one would expect an additional p-wave contribution. The angular distributions for the processes

$\sigma_v(v=0\rightarrow 4;\ \Delta j=0)$ and $\sigma_{rv}(v=0\rightarrow 4;\ j=1\rightarrow 3)$

are presented in Fig. 11. Whereas the total vibrational cross section $\sigma_{v+rv}(\vartheta)$, which had been determined in earlier measurements [5] and can also be

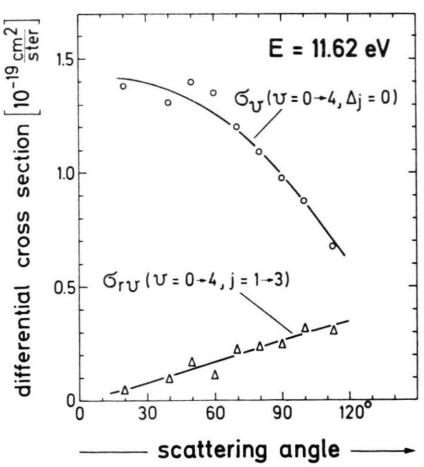

Fig. 11.. Measured angular distributions in absolute units for the processes σ_v $(v=0\rightarrow 4;\ \Delta j=0)$ and σ_{rv} $(v=0\rightarrow 4;\ j=1\rightarrow 3)$ at a colliison energy of $E=11.62$ eV (nearly pure resonance scattering). The anisotropy of σ_v and the existence of σ_{rv} cannot be explained by pure s-wave scattering.

calculated from the data of Fig. 11, is much more isotropic and supports the first order approximation of pure s-wave scattering for the resonance process, the results of Fig. 10 and 11 demonstrate the importance of investigating the processes σ_v and σ_{rv} separately.

The experimental errors for the differential cross sections of Fig. 11 are roughly 20% in arbitrary units and about 30% in absolute units and become still larger for the smaller values of $\sigma_{rv}(\vartheta)$. The absolute values have been corrected for the finite energy resolution of the apparatus. – The results concerning the direct excitation process at $E=10.8$ eV have already been presented in Fig. 5 and in Tables 3 and 4.

Conclusions

In a beam experiment, the proceses of elastic scattering, pure rotational excitation and deexcitation, pure vibrational excitation, and simultaneous rotational and vibrational excitation have been investigated for $e-H_2$ scattering in the energy range from 0.3 eV up to the 12 eV region where Feshbach-resonances become important for the collision processes. Differential and integral cross sections have been determined in arbitrary and in absolute units for all processes. Differential cross sections give better insight into details of the scattering process than integral and total cross sections. They are more sensitive to small contributions of unexpected or underestimated partial waves and allow more detailed comparison with theory. A partial wave analysis of the differential cross sections should be very useful for the increasing refinement of the ab-initio calculations.

Particularly, in this work different excitation mechanisms have been investigated for rotational and vibrational excitation of H_2 by slow electron impact:

a) The energy range below 10 eV can be described by the superposition of a very broad $^2\Sigma_u^+$-shape resonance near 3 eV on a background of direct scattering. A shape resonance is always connected with partial waves $l>0$. Therefore, this type of resonance is equally effective for rotational and for vibrational excitation. It is clear that this conclusion holds in the same way for the well known shape resonances in other molecules (N_2, CO etc.), where rotational transitions could not be resolved until now. The separation into pure vibrational and simultaneous rotational-vibrational excitation has

proved to be very useful. The discrepancy in $\sigma_{v+rv}(\vartheta)$ between theory and experiment in the earlier investigations is found to be mainly due to $\sigma_v(\Delta j=0)$, while $\sigma_{rv}(\vartheta)$ agrees quite well.

b) The energy range around 12 eV is characterized by the superposition of direct scattering and Feshbach-resonances. It has been discussed that in the case of H_2 Feshbach-resonances may be expected to have $^2\Sigma_g^+$-configuration in most cases. For the decay into the electronic ground state of H_2, which is of interest here, the dominating partial wave is the s-wave. This type of resonance is effective for vibrational excitation, but less important for rotational excitation. Obviously, this conclusion depends on the configuration of the resonant state and of the final state of the molecule.

c) The direct scattering process is present as a background process in the whole energy range. The direct scattering amplitude normally contains several partial waves, so that one finds direct rotational as well as direct vibrational excitation. Usually, the angular distributions vary with energy much more rapidly than in the case of the resonance scattering mechanism. The relative importance of the direct scattering amplitude is decreasing with increasing quantum number of the exit channel ($v=0$ for elastic scattering; $v=1, 2, 3, \ldots$ for vibrational excitation). The contributions to elastic scattering are relatively large, the cross sections for rotational and vibrational excitation due to direct scattering are very small. — These findings are expected to be valid also for other molecules.

Acknowledgements

We would like to thank Prof. Dr. H. EHRHARDT for encouragement and stimulating discussions. The e−He data of D. ANDRICK and A. BITSCH were of great use for the measurements of this work. The help of M. EYB in performing angular distribution measurements is also greatfully acknowledged.

Experimental Study of Low Energy e-O_2 Collision Processes

F. LINDER and H. SCHMIDT

Fachbereich Physik der Universität Trier-Kaiserslautern

(Z. Naturforsch. **26 a**, 1617—1625 [1971]; received 1 July 1971)

Elastic scattering, vibrational excitation to $v=1$, 2, 3, 4 of the electronic ground state, and electronic excitation to the states $a^1\Delta_g$ and $b^1\Sigma_g^+$ of O_2 have been measured in a crossed beam apparatus for collision energies from nearly 0 eV to 4 eV. Differential and integral cross sections have been determined and calibrated on an absolute scale. From 15 vibrational levels of O_2^-, which could be observed as resonances in the cross sections, the spectroscopic constants for the vibrational structure of O_2^- have been derived: $\omega_e = 135$ meV and $\omega_e x_e = 1$ meV. The cross sections for vibrational excitation have the order of 10^{-18} cm². eV for the larger resonance peaks. Detailed cross sections have been listed in Table 1. The half width of the resonance can be estimated to $\Gamma \approx 0.5$ meV, which corresponds to a lifetime tof 10^{-12} sec for the O_2^- states. The angular dependence of pure resonance scattering is rather flat and not in accordance with the simplest theoretical model. An analysis of the angular dependence and of the rotational structure of the resonance in a somewhat extended model have been performed. — No electronically excited O_2^- states could be detected in the energy range up to 3 eV.

Introduction

Low energy e − O_2 collision processes are of special interest in high atmosphere physics. In a more general context, the e − O_2 system represents an interesting example for the study of reaction mechanisms of electron-molecule scattering. It is well known that higher vibrational states of O_2^-, which is a stable negative ion in its lower vibrational levels, play an important role in electron scattering processes at very low energies. The formation and decay of these resonant states can be explained within the frame of the Born-Oppenheimer approximation. They are interpreted as very low-lying shape resonances [1a] in contrast to an earlier interpretation as nuclear-excited Feshbach resonances [1b]. Because of the low resonance energies and the high centrifugal barrier these resonances show characteristic differences compared with other resonance types which are discussed in the preceding paper [2].

Reprints request to Dr. F. LINDER, NOAA Environmental Research Laboratories, *Boulder, Colorado 80302*, USA.

[1a] A. HERZENBERG, J. Chem. Phys. **51**, 4942 [1969].

[1b] J. N. BARDSLEY and F. MANDL, Reports on Progress in Physics **31**, 471 [1968].

[2] F. LINDER and H. SCHMIDT, Z. Naturforsch. **26 a**, 0000 [1971]; preceding paper.